



# Qing Xia Jie Yi Formula granules alleviated acute pancreatitis through inhibition of M1 macrophage polarization by suppressing glycolysis

Xiao Han<sup>a,b,1</sup>, Jingpiao Bao<sup>a,b,1</sup>, Jianbo Ni<sup>a,b</sup>, Bin Li<sup>a,b</sup>, Pengli Song<sup>a,b</sup>, Rong Wan<sup>a,b</sup>, Xingpeng Wang<sup>a,b</sup>, Guoyong Hu<sup>a,b,\*\*</sup>, Congying Chen<sup>a,b,\*</sup>

<sup>a</sup> Department of Gastroenterology, Shanghai General Hospital, Shanghai Jiao Tong University School of Medicine, Shanghai, China

<sup>b</sup> Shanghai Key Laboratory of Pancreatic Disease, Institute of Pancreatic Disease, Shanghai Jiao Tong University School of Medicine, Shanghai, China

## ARTICLE INFO

Handling Editor: Dr. K Shaari

### Keywords:

Acute pancreatitis  
Macrophage polarization  
Qing Xia Jie Yi Formula granules  
Glycolysis  
Lung injury

## ABSTRACT

**Ethnopharmacological relevance:** Herbal formulas from Traditional Chinese Medicine are common and well-established practice for treating acute pancreatitis (AP) patients. However, little is known about their bioactive ingredients and mechanisms, such as their targets and pathways to inhibit inflammation.

**Aim of the study:** This study aimed to evaluate the effect of Qing Xia Jie Yi Formula (QXJYF) granules on AP and discuss the molecular mechanisms involved.

**Materials and methods:** Major compounds in QXJYF granules were identified using UPLC-quadrupole-Orbitrap mass spectrometry (UPLC-Q-Orbitrap MS). The effect of QXJYF granules on experimental AP models both *in vitro* and *in vivo*, and detailed mechanisms were clarified. Two AP models were induced in mice by intraperitoneally injections of caerulein or L-arginine, and QXJYF granules were used to treat AP mice *in vivo*. Histological evaluation of pancreas and lung, serum amylase and lipase levels, serum inflammatory cytokines, inflammatory cell infiltration and macrophage phenotype were assessed. Bone marrow derived macrophages (BMDMs) were cultured and treated with QXJYF granules *in vitro*. BMDM phenotype and glycolysis levels were measured. Lastly, clinical effect of QXJYF granules on AP patients was verified. Predicted severe AP (pSAP) patients eligible for inclusion were assessed for enrollment.

**Results:** Nine major compounds were identified in QXJYF granules. Data showed that QXJYF granules significantly alleviated AP severity both in caerulein and L-arginine-induced AP models *in vivo*, pancreatic injury and inflammatory cell infiltration, systematic inflammation, lung injury and inflammatory cell infiltration were all improved after QXJYF treatment. QXJYF granules significantly reduced M1 macrophages during AP both *in vivo* and *in vitro*; besides, the mRNA expression levels of M1 genes such as *inos*, *Tnfα*, *Il1β* and *Il6* were significantly lower after QXJYF treatment in M1 macrophages. Mechanistically, we found that *HK2*, *PFKFB3*, *PKM*, *LDHα* levels were increased in M1 macrophages, but significantly decreased after QXJYF treatment. Clinical data indicated that QXJYF granules could significantly reduce CRP levels and shorten the duration of organ failure, thereby reducing the incidence of SAP and preventing pSAP patients from progressing to SAP.

**Conclusion:** QXJYF granules alleviated AP through the inhibition of M1 macrophage polarization by suppressing glycolysis.

## 1. Introduction

Acute pancreatitis (AP) is a common inflammatory disease of the exocrine pancreas that affects human life and health, with a global

morbidity of approximately 30–40 per 100,000 people (Szatmary et al., 2022). The mortality rate of AP is about 3–10%, while the mortality rate of severe AP (SAP) increases to 36–50% (Lee and Cho, 2022). Due to the pathological mechanisms have not been fully elucidated, no effective

\* Corresponding author. Department of Gastroenterology, Shanghai General Hospital, Shanghai Jiao Tong University School of Medicine, 100 Haining Road, Shanghai, 200080, China.

\*\* Corresponding author. Department of Gastroenterology, Shanghai General Hospital, Shanghai Jiao Tong University School of Medicine, 100 Haining Road, Shanghai, 200080, China.

E-mail addresses: [guoyong.hu@shgh.cn](mailto:guoyong.hu@shgh.cn) (G. Hu), [congyin.chen@shgh.cn](mailto:congyin.chen@shgh.cn) (C. Chen).

<sup>1</sup> These authors contributed equally to this work.

<https://doi.org/10.1016/j.jep.2024.117750>

Received 6 November 2023; Received in revised form 28 December 2023; Accepted 9 January 2024

Available online 10 January 2024

0378-8741/© 2024 Elsevier B.V. All rights reserved.

treatment is available. Tissue damages including toxic injuries, infection and other causes induce macrophages to drive inflammatory responses. Premature activation of trypsinogen in pancreatic acinar cells leads to autodigestion of the pancreas and release of proinflammatory cytokines (Cruz and Rohban, 2020). Proinflammatory cytokines such as TNF $\alpha$ , IL1 $\beta$ , IL6 and CCL2 recruit monocytes and macrophages to the pancreas and amplify inflammatory response (Wu et al., 2020). Macrophages can be divided into M1 and M2 subtypes based on different stimuli and function *in vitro*. However, the polarization status of macrophages in pancreatic tissue is affected dynamically by the complex local micro-environment (Manohar et al., 2021). Several studies illustrate a dynamic phenotype of macrophages during AP: M1-type macrophages dominated in the acute inflammatory phase of AP, while M2 macrophages dominated during the process of pancreas repair or regeneration (Wu et al., 2020). If the recruitment or activation of monocytes and macrophages is blocked, the inflammatory response following tissue injury is often diminished and the severity of AP also ameliorated. Therefore, the strategies intervening monocyte and/or macrophage infiltration or activation could be a novel potential tool for treating AP, which still has no specific treatment.

Accumulating evidence has revealed that cellular metabolic adaptation is an important characteristic of macrophage to support the different polarization status and its functions (Yuan and Fan, 2022). For example, M1 macrophages require glucose and aerobic glycolysis; in contrast, in response to IL4, M2 macrophages majorly metabolize fatty acids and depend on oxidative phosphorylation. These metabolic changes are the result of cytokine stimulation but can also determine macrophage function and phenotype (Edgar and Akbar, 2021). Furthermore, recent reports have highlighted the vital role of aerobic glycolysis in activated macrophages, which switch their metabolic pathway from oxidative phosphorylation to aerobic glycolysis (Edgar and Akbar, 2021). Therefore, genetic or pharmacological intervention of aerobic glycolysis can regulate the phenotype of macrophages. Glycolysis is a series of reactions consisting of a ten-step process that begins with a single glucose molecule and ends up with two pyruvate molecules, involving several rate-limiting enzymes including Hexokinase 2 (HK2), Fructose-2, 6-diphosphatase 3 (PFKFB3), pyruvate kinase (PKM) and lactic dehydrogenase  $\alpha$  (LDH $\alpha$ ) (Naifeh et al., 2023). However, the specific mechanisms and target of glycolysis regulating macrophage polarization during AP have not been fully elucidated.

Traditional Chinese Medicine (TCM) herbal formulas are commonly used to treat AP patients, with Dachengqi decoction or Qing Yi decoction all being common prescriptions (Wen et al., 2020). Several studies have shown that bioactive ingredients such as emodin, baicalin and honokiol can significantly reduce experimental AP severity by suppressing pro-inflammatory mediators, and improving clinical outcomes of AP patients (Yang et al., 2020). Qing Xia Jie Yi Formula (QXJYF) granules are an improved prescription modified from Qing Yi Decoction which has been used for SAP for many years with satisfactory clinical efficacy in China (Wei et al., 2021). It could reduce infection rates and restore gastrointestinal motility among SAP patients (Chen et al., 2015). However, the individual ingredients, the exact action and mechanisms of QXJYF granules on AP, and effect on SAP incidence of pSAP patients remain to be clarified. Recent studies have shown that Qing Yi Decoction may alleviate AP severity by inhibiting inflammation and promoting apoptosis (Wei et al., 2021). However, the effect of QXJYF granules on macrophage phenotype have not been reported. In this study, we investigated the effect of QXJYF granules on AP and explored the underlying mechanisms by regulating macrophage phenotype through modulating glycolysis.

## 2. Materials and Methods

### 2.1. Preparation of QXJYF granules

The herbs of QXJYF granules were provided by Chinese Herbs

Pharmacy of Shanghai General Hospital (Shanghai, China), including Rhubarb (*Rheum palmatum* L.) 15 g, Unripe bitter orange (*Citrus aurantium* L.) 12 g, caulis sargentodoxae (*Sargentodoxa cuneata* (Oliv.)) 30 g, Gardenia fruit (*Gardenia jasminoides* J.Ellis) 9 g, Chinese tho rowax root (*Bupleurum marginatum* Wall. ex DC.) 9 g, Corydalis Rhizoma (*Corydalis yanhusuo*) 12 g, Chinese red sage (*Salvia miltiorrhiza* Bunge) 15 g, Paeoniae Radix Rubra (*Paeonia lactiflora* Pall.) 15 g. The plants' name has been checked in <http://mpns.kew.org>. The above-mentioned herbs were respectively placed in a decocting pot, soaked with water for about 1 cm of crude herbs, soaked for half an hour, then boiled at a gentle fire for 15 min, slag removed, and concentrated to 1 g of crude drugs per milliliter, finally, lyophilized into granules. Store at room temperature and before administration to animals, the QXJYF granules were dissolved in normal saline with a concentration of 0.16 g/ml.

### 2.2. UPLC-quadrupole-Orbitrap mass spectrometry (UPLC-Q-Orbitrap MS) analysis

To find out the major ingredients of QXJYF granules, Hypersil GOLD aQ C18 column (100 mm  $\times$  2.1 mm, 1.9  $\mu$ m, Thermo Fisher) using a Dionex Ultimate 3000 RSLC system (Thermo Fisher) which is equipped with a photodiode array detector, a quaternary gradient pump, and an autosampler, was used to perform fingerprint spectrum for QXJYF granules. The components were eluted with a gradient system that contains 0.1 % formic acid (mobile phase A) and LC-MS grade acetonitrile (mobile phase B; time, min/B%: 0/1, 5/95, 50/40, 55/75 and 57/1). The chromatographic column used was ThermoHypersil GOLD (100  $\times$  4.6 mm). The column temperature was maintained at 30  $^{\circ}$ C and the mobile phase flow rate was 0.3 mL/min. 7 g of extract samples were re-dissolved in 35 mL of methanol, and ultrasonic extracted for 40 min. The solution was centrifuged at 15,000 r/min for 15 min, and the supernatant was collected, then filtered through a 0.22  $\mu$ m filter before analysis. To prepare the standard solution, 9 standards (Chlorogenic acid, Geniposide, Albiflorin, Protopine, Naringin, Neohesperidin, Rotundine, Dehydrocorydaline, Emodin; Chengdu must biotechnology, Sichuan, China) were dissolved in methanol.

The sample was scanned in Full MS-ddMS2 mode using an ESI ion source with positive and negative ion switching, and primary and secondary mass spectra were acquired. The optimized mass spectrometry parameters were as follows: sheath gas flow rate of 45 arb; auxiliary gas flow rate of 15 arb; capillary temperature of 320  $^{\circ}$ C; MS1 resolution of 70,000; MS/MS resolution of 17,500; NCE model collision energy of 20/40/60 eV; and voltage of 3.8 kV (positive mode) or -3.1 kV (negative mode).

### 2.3. Mouse strains

C57BL/6J mice (aged 6- to 8- week-old, weighed 20–22g, male) were purchased from Shanghai Model Organisms Center Inc. (Shanghai, China). Before the experiment, all the mice were fed in individually ventilated cages (4–6 mice per cage) under specific-pathogen-free conditions at 22  $\pm$  2  $^{\circ}$ C and a 12 h dark/light cycle with free access to a standard rodent diet and water. All mice were randomly divided into each group (n = 9 per group). All the experiments involving animals were approved by the Animal Ethics Committee of Shanghai General Hospital (2020AW102).

### 2.4. Experimental AP models and treatments

Two widely used, rapidly induced and noninvasive experimental AP models were built *in vivo* (Lerch and Gorelick, 2013). One model was induced by hourly intraperitoneally injections of caerulein (100  $\mu$ g/kg, for ten injections) as reported before (Sah et al., 2013; Wen et al., 2015). The first injection of caerulein was defined as 0 h. Control mice received equal normal saline (NS) instead of caerulein. The QXJYF granules (4.8



mg/g, 0.6 ml) was administered intragastrically (i.g) for 3 times, at 3 h, 5 h and 7 h after the first caerulein injection respectively, and mice were euthanized at 12 h. The other model was induced by hourly intraperitoneally injections of L-arginine (L-arg, 4 g/kg, 8%, pH = 7.0, for two injections) as previously described (Dawra et al., 2007). The second injection of L-arginine was defined as day 0. Controls received NS equivalent to L-arginine. QXJYF granules (4.8 mg/g, 0.6 ml) was divided into two equal doses intragastrically, 2 h before and 1 h after the first L-arginine injection respectively, and equivalent QXJYF granules was added every day in the following two days. Mice were sacrificed at day 3. Serum, pancreas and lung tissues were collected. Histological scoring of pancreas hematoxylin and eosin (H&E) sections were performed by two blind independent experienced pathologists, graded from 0 to 3 for edema, inflammation, and necrosis (Han et al., 2022; Van Laethem et al., 1995).

## 2.5. Serological test

Serum was collected from blood samples which were centrifuged at 400 g for 20 min at 4 °C to acquire serum. The activities of amylase and lipase were measured by a Roche/Hitachi Modular Analytics System (Roche, Basel, Switzerland) in accordance with the manufacturer's instructions. Serum concentrations of TNF $\alpha$ , IL6, IL1 $\beta$ , CCL2 and CXCL2 were measured using Enzyme linked immunosorbent assay (ELISA) kits and following the manufacturer's protocols (Westang bio-tech Co, LTD, Shanghai, China).

## 2.6. Hematoxylin and eosin (H&E) and immunohistochemical staining

Mice pancreas and lung tissues were fixed in 4 % neutral paraformaldehyde for 24–48 h at room temperature. Afterward, they were embedded in paraffin and then cut into 4  $\mu$ m sections for H&E staining by standard procedures. To ensure accurate results, the endogenous peroxidase was neutralized by a 3 % hydrogen peroxide solution. The sections were then incubated with monoclonal antibody against F4/80 (diluted to 1:100) or Ly6G (diluted to 1:100) at 4 °C overnight. After being washed in PBS for three times, the sections were incubated with secondary antibody for 1 h. Finally, the sections were imaged using an ultrasensitive SP kit and a DAB kit (provided by Fuzhou Maxin, China) at 37 °C. The pancreatic tissue sections were graded on a scale of 0–3, with 0 representing a normal appearance and 3 indicating severe for edema, inflammation and necrosis (Han et al., 2022; Kim et al., 2015).

## 2.7. Immunofluorescence staining

Fresh pancreas specimens were fixed in 4 % neutral paraformaldehyde for 2 h. They were then dehydrated overnight in 30 % sucrose, embedded in OCT, and processed into 4  $\mu$ m thickness slices. The slices were then incubated at 4 °C overnight with polyclonal antibodies against iNOS (1:400) or CD206 (1:200), and F4/80 (1:1500). After being washed in PBS for three times, the slices were incubated with Try-488 or Try-cy3 (runnerbio, China) labeled Goat anti-rabbit IgG H&L (HRP) (1:2000, abcam, USA) for 45 min in the dark. Finally, antifade mounting medium with 2-(4-Amidinophenyl)-6-indolecarbamidine dihydrochloride (DAPI; Beyotime Biotechnology, China) was used to seal the slices. Immunofluorescence staining results were analyzed using a laser scanning confocal microscope (LSCM; Zeiss, Germany).

## 2.8. Murine bone marrow derived macrophage preparation

*In vitro*, bone marrow derived macrophages (BMDMs) were isolated and cultured according to previously described methods (Anthony et al., 2011; Ying et al., 2013). In brief, bone marrow cells were collected from femurs and tibias of C57BL/6J mice. After removing the red blood cells, bone marrow cells were resuspended in Dulbecco's modified Eagle's medium/Ham (DMEM) F-12 medium with 20 ng/mL rmM-CSF and 10 %

fetal bovine serum. Nonadherent cells were removed on day 3. CD11b<sup>+</sup>F4/80<sup>+</sup> macrophages were identified using flow cytometry on day 6. M1 macrophages were induced by LPS (100 ng/mL) and IFN $\gamma$  (10 ng/mL) with or without QXJYF (0.5, 1 mg/mL) treatment for 24h simultaneously with LPS and IFN $\gamma$ .

## 2.9. Flow cytometry

All mouse flow antibodies were purchased from Thermo Fisher Scientific (Waltham, MA, USA). For intracellular TNF $\alpha$  staining, cells were incubated with LPS (100 ng/mL) and brefeldin A (3  $\mu$ g/mL, Thermo Fisher Scientific, Waltham, MA, USA) at 37 °C for 3 h before surface staining (Xue et al., 2015). The cells were then processed by the Intracellular Fixation & Permeabilization Buffer Set (Thermo Fisher Scientific, Waltham, MA, USA) according to the instructions. Finally, BMDMs were stained with the following antibodies: APC-iNOS (17–5920, 1:100) and isotype control (17-4321-81, 1:200), APC-TNF $\alpha$  (17-7321-81, 1:100) and isotype control (17-4301-82, 1:200). FACSCanto II (BD Biosciences, Franklin, NJ, USA) was used to perform flow cytometry and the results were analyzed with FlowJo software (Tree Star Inc., OR, USA).

## 2.10. Western blotting

Total protein was extracted according to the previous method (Han et al., 2022). Proteins (40  $\mu$ g per lane) were separated by 10 % SDS-PAGE and transferred to nitrocellulose membranes (Millipore, Mass, USA). The membranes were next incubated with primary antibodies against monoclonal HK2 (1:1000), PFKFB3 (1:1000), PKM (1:10000), LDH $\alpha$  (1:1000) and  $\beta$ -actin (1:800) overnight at 4 °C. Following that, the membranes were probed with HRP-labeled second antibodies for 1 h at 37 °C. Finally, the membranes were scanned using an image analyzer and visualized with an ECL kit (Millipore, #WBKLS0100). To ensure control of potential sources of variation, the relative expression of proteins was normalized to  $\beta$ -actin in different experimental groups. The value of control group was set as 1, and the values of the other groups were compared to the control group value, represented as fold changes relative to the control values.

## 2.11. Quantitative reverse transcription polymerase chain reaction (qRT-PCR)

BMDM mRNA transcripts were analyzed by qRT-PCR. Total RNA was extracted from BMDMs with Trizol reagent (Invitrogen, CA, USA). The RNA was then reverse transcribed using the PrimeScript<sup>TM</sup> RT reagent kit (Takara Bio, Kusatsu, Japan). Primers used in the qRT-PCR can be found in [Supplementary Table 1](#). All the experimental procedures were conducted using SYBR<sup>®</sup> Premix Ex Taq<sup>TM</sup> (Takara Bio, Kusatsu, Japan) and the applied biosystems (Life technologies, CA, USA) following the provided instructions. To calculate the fold changes for each gene, the comparative CT ( $2^{-\Delta\Delta CT}$ ) method was employed. In order to control for any sources of variation, the relative expression of mRNA levels was normalized to the  $\beta$ -actin mRNA expression in different groups. The expression value in the control group was set to 1, and the values of the other groups were compared to the control group value, presented as fold change relative to the control values. Each gene was repeated three times in each experiment to ensure reproducibility and reliability.

## 2.12. AP patient recruitment and treatment

To evaluate the impact of early application of QXJYF granules on the severity and progression of AP patients, predicted severe AP (pSAP) patients aged 18–75 admitted within 48 h of onset who admitted to the Department of Gastroenterology, Shanghai General Hospital, Shanghai Jiao Tong University School of Medicine from August 2020 to July 2021 will be assessed for enrollment. We included those pSAP patients

conformed to any of the following criteria while meeting the AP diagnostic criteria: (1) APACHE II score  $\geq 8$ ; (2) BISAP score  $\geq 3$ ; (3) PASS score  $>140$ ; (4) CRP  $>150$  mg/mL (Buxbaum et al., 2018; Vege et al., 2015). Patients with any of the following conditions were excluded: (1) pregnant or lactating at admission; (2) combined with malignant tumor or having radiotherapy and chemotherapy within 6 months; (3)

combined with gastrointestinal perforation, bleeding or mechanical ileus at admission; (4) acute attack of chronic pancreatitis; (5) known history of neoplasm in duodenal or biliopancreatic systems; (6) history of pancreatic resection; (7) undergoing other clinical trials; (8) taking traditional Chinese medicine (TCM) orally before enrolment. AP severity was assessed by Atlanta classification 2012 (Banks et al., 2013).

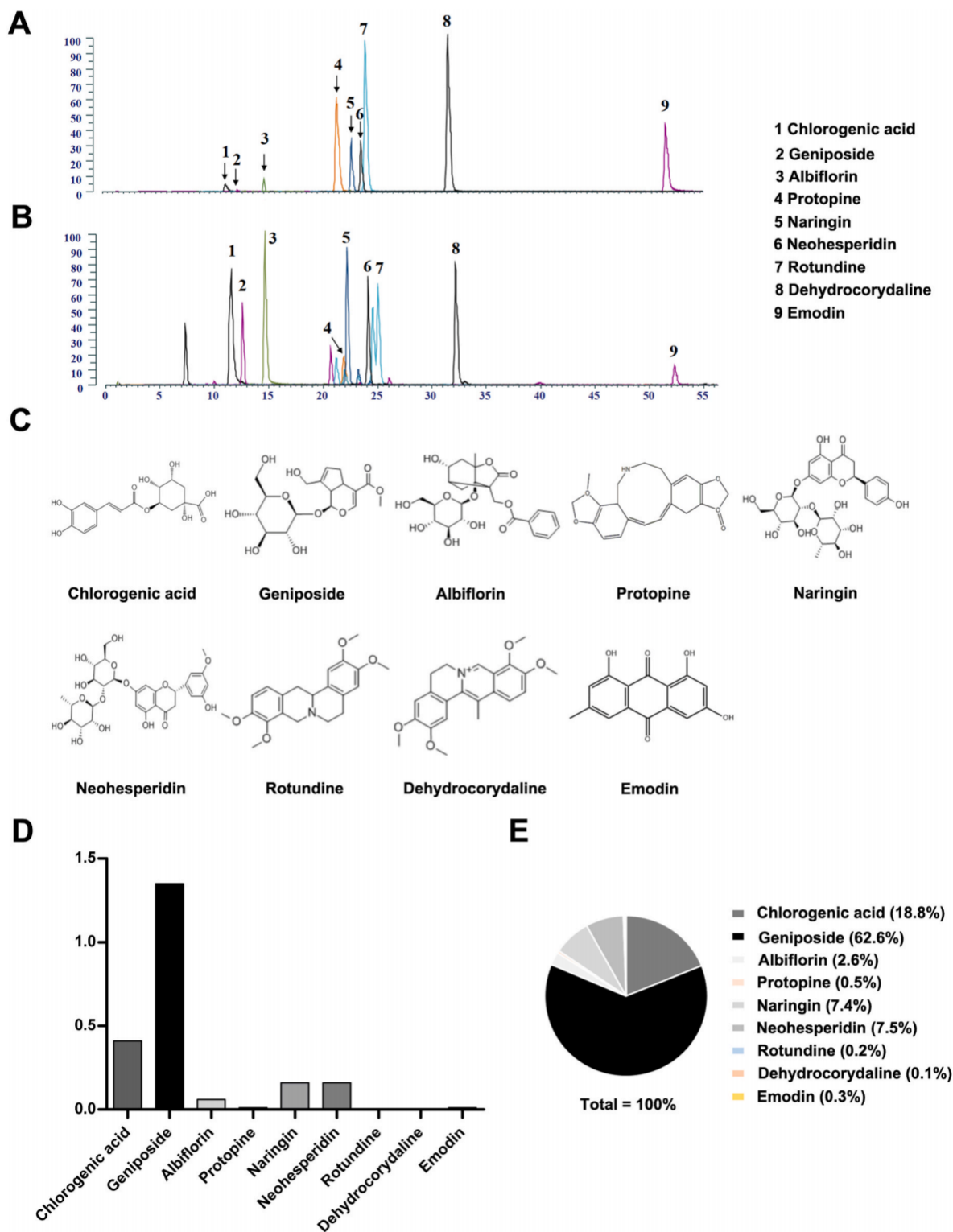


**Fig. 1.** Extraction ion flow chromatogram of 9 major ingredients in QXJYF granules. (A) Mixed standards; (B) QXJYF sample; (C) Chemical structure of chlorogenic acid, geniposide, albiflorin, protopine, naringin, neohesperidin, rotundine, dehydrocorydaline and emodin; (D) The content of 9 major ingredients in QXJYF granules; (E) The percentage of each active ingredient in the total 9 major ingredients.



psAP patients were randomly divided into treatment group and control group, the control group was given conventional comprehensive medical treatment, and the treatment group was given QXJYF granules (0.16 g/mL, 100 mL, twice daily, p.o., for 7 days) on the basis of the control group. The clinical data of AP patients were all obtained, including age, gender, severity, etiology, BMI, CRP levels, PASS score, SIRS and APACHE II score, etc. Patient-informed consent was obtained according to the study protocol, which was approved by the ethics committee of Shanghai General Hospital (No. 2020 [66]). This prospective, placebo-controlled and randomized trial was registered on the Chinese Clinical Trial Registry (<https://www.chictr.org.cn/>, ID: ChiMCTR200003894).

### 2.13. Statistical analysis

Continuous variables were presented as mean  $\pm$  standard deviation (SD). Frequency and percentage (%) were used to describe categorical data. In cases where the data followed a Gaussian distribution, parametric tests such as Student's t-test for two groups, or one-way ANOVA for three groups were conducted. If the data were not normally distributed, non-parametric tests like Mann-Whitney test for two groups or Kruskal-Wallis test with Dunn's post test for three groups were employed. The  $\chi^2$  test was used for counting data, and the Fisher exact test was used when necessary. All analyses were performed using SPSS 17.0 Software (SPSS, Inc., Chicago, IL, USA). A significant level of  $P$  value  $< 0.05$  was considered statistically significant. The experimental results were acquired from at least three independent experiments, each consisting of at least three mice per group, in order to ensure the accuracy of the findings.

### 2.14. Reagents

Lipopolysaccharide (LPS; cat # L2880), caerulein (Cae; cat # C9026) and L-arginine (L-Arg; cat # A5131) were purchased from Sigma-Aldrich Chemical (St. Louis, MO, USA). Antibodies against HK2 (cat # 2867) were from Cell Signaling Technology (Danvers, MA, USA). Antibodies against PFKFB3 (cat # ab181861), PKM (cat # ab150377) were from Abcam (Cambridge, MA, USA). Antibodies against LDH $\alpha$  (cat # 19987-1-AP) were from Proteintech Biotechnology (Wuhan, China).

## 3. Results

### 3.1. Identification of the major compounds in QXJYF granules by UPLC-Q-Orbitrap MS

To ensure the consistency and quality control of QXJYF granules manufacture, major compounds of QXJYF granules were identified with UPLC-Q-Orbitrap MS. As shown in Fig. 1A and B, the baseline of the mixed QXJYF granules sample and standard solution were stable, and chromatographic peaks of ingredients were separated. Comparing the retention time, and MS spectra with reference samples, 9 major components were identified: chlorogenic acid, geniposide, albiflorin, protopine, naringin, neohesperidin, rotundine, dehydrocorydaline and emodin. The sum of chlorogenic acid and geniposide in QXJYF granules accounted for 81.42 % of the total content of the 9 major ingredients (Fig. 1C–E). However, they only made up 0.0022 % of the total QXJYF granules.

### 3.2. QXJYF granules alleviated pancreas injury during AP

Several studies have indicated that single component such as chlorogenic acid (Tarasiuk et al., 2021), geniposide (Zhang et al., 2019), albiflorin, protopine, naringin, neohesperidin (Bi et al., 2023) or emodin (Wu et al., 2022) can ameliorate AP or AP-associated lung injury via inhibition of inflammation, oxidative stress or cell death. In our study, we focused on the effect and mechanisms of their combination in QXJYF

granules other than individual compound alone, highlighting their synergistic effect during AP. In order to thoroughly investigate the effects of QXJYF granules on AP, we conduct experiments using a caerulein-induced AP model in C57BL/6J mice with or without QXJYF granules treatment. To evaluate the severity of pancreatic injury, we performed histological examination at 12 h. The results showed that QXJYF-treated mice exhibited significantly less severe pancreatic injury compared to the AP group, and the histological scores showed remarkable improvement after QXJYF treatment (Fig. 2A and B). Furthermore, we measured levels of serum amylase and lipase activities, which were key indicators of pancreatic function. Data showed that QXJYF-treated mice demonstrated markedly decreased amylase and lipase activities compared to the AP group (Fig. 2C). To gain further insights into the mechanism behind these effects, we examined the infiltration of F4/80 $^{+}$  macrophages and Ly6G $^{+}$  neutrophils in the pancreatic tissue using immunohistochemistry staining. The data clearly indicated that QXJYF granules reduced the infiltration of F4/80 $^{+}$  macrophages and Ly6G $^{+}$  neutrophils in the pancreas, as compared to the AP group (Fig. 2D and E). To validate the robustness of our findings, we also conducted experiments using an L-arginine-induced AP model. Remarkably, similar results were obtained at day 3, pancreatic injury and histological scores, serum amylase and lipase levels, F4/80 $^{+}$  macrophage and Ly6G $^{+}$  neutrophil infiltration were all improved after QXJYF treatment, as shown in Fig. 3A–E. To be specific, QXJYF treatment demonstrated a significant alleviation of pancreatic injury, including histological improvement, reduction in histological scores, impaired serum amylase and lipase activities, and decreased infiltration of F4/80 $^{+}$  macrophages or Ly6G $^{+}$  neutrophils in the pancreatic tissue during L-arginine-induced AP. In summary, our findings strongly suggested that QXJYF granules had a profound protective effect against pancreatic injury both in caerulein and L-arginine-induced AP models *in vivo*.

### 3.3. QXJYF granules alleviated systemic injury during AP

To further investigate the effect of QXJYF granules on systemic injury during AP, caerulein and L-arginine-induced AP models in C57BL/6J mice were built. The mice were treated with or without QXJYF granules, and serum levels of inflammatory cytokines and lung injury were assessed *in vivo*. On the one hand, we observed a significant decrease in the serum levels of inflammatory cytokines such as TNF $\alpha$ , IL1 $\beta$  and IL6 in QXJYF-treated mice compared to the AP groups both in caerulein and L-arginine-induced AP models (Fig. 4A and E). On the other hand, the lung tissues of the groups treated with QXJYF granules exhibited significantly alleviated morphological changes compared to the AP groups (Fig. 4B and F). In addition, to further evaluate the effects of QXJYF granules on immune cell infiltration in the lung tissue, we performed immunohistochemistry staining for F4/80 (a macrophage marker) and Ly6G (a neutrophil marker) respectively. Data showed a significant reduction in F4/80 $^{+}$  macrophage and Ly6G $^{+}$  neutrophil infiltration in the lung tissue of the mice treated with QXJYF granules compared to the AP groups (Fig. 4C,D,G,H). Overall, these findings indicated that QXJYF granules significantly alleviated systemic injury both in caerulein and L-arginine-induced AP models *in vivo*.

### 3.4. QXJYF granules inhibited M1 macrophages during AP

Several studies have shed light on the dynamic phenotype of macrophages during AP. It has been observed that M1-type macrophages dominated in the acute inflammatory phase of AP, while M2 macrophages took over during the process of pancreas repair or regeneration. Understanding of the macrophage dynamics in AP has opened up new avenues for exploring the mechanisms of the disease and identifying potential targets for novel therapeutic strategies (Wu et al., 2020). Therefore, caerulein or L-arginine-induced AP model in C57BL/6J mice was built with or without QXJYF granules treatment, then we examined the infiltration of F4/80 $^{+}$ iNOS $^{+}$  M1 macrophages and F4/80 $^{+}$ CD206 $^{+}$



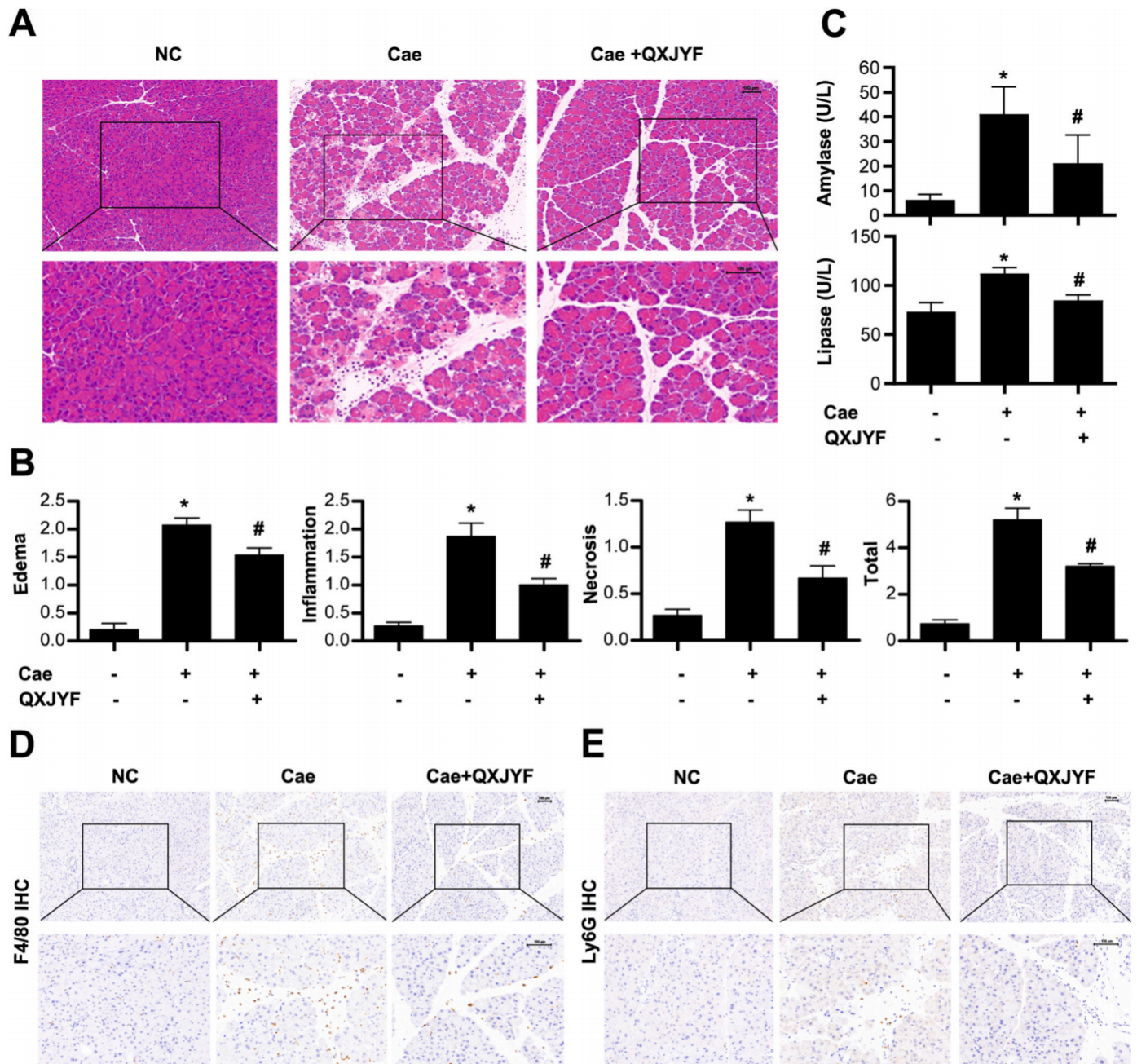


**Fig. 2.** QXJYF granules alleviated pancreas injury in caerulein-induced AP model. *In vivo*, AP was induced by injection of caerulein (100 µg/kg) in C57BL/6J mice, and treated with QXJYF granules (4.8 mg/g, 0.6 ml, i.g.; at 3 h, 5 h and 7 h after the first caerulein injection respectively). (A) Representative micrographs of H&E-stained pancreatic sections (100 × (up) and 200 × (down)); (B) Histological scores were determined as described in Methods; (C) Change in serum activity of amylase (up) and lipase (down); (D) Representative micrographs of macrophage marker F4/80 immunohistochemical analyses in pancreas (100 × (up) and 200 × (down)); (E) Representative micrographs of neutrophil marker Ly6G immunohistochemical analyses in pancreas (100 × (up) and 200 × (down)). All experiments were performed at least three times. Data are presented as Mean ± SEM. n = 9 per group. Scale bar = 100 µm \*P < 0.05 versus NC, #P < 0.05 versus AP. Cae, caerulein; NC, normal control; QXJYF, Qing Xia Jie Yi Formula; i.g, intragastrical administration.

M2 macrophages in the pancreatic tissue by immunofluorescence staining. The results revealed that QXJYF granules significantly inhibited the presence of F4/80<sup>+</sup>iNOS<sup>+</sup> M1 macrophages, while promoting the abundance of F4/80<sup>+</sup>CD206<sup>+</sup> M2 macrophages in the pancreatic tissue, and this effect was observed both in the caerulein and L-arginine-induced AP models *in vivo* (Fig. 5A–D). In order to further elucidate the role of QXJYF granules on macrophage polarization, we isolated and cultured BMDMs from C57BL/6J mice. These BMDMs were stimulated towards M1 phenotype by LPS (100 ng/mL) and IFN $\gamma$  (10 ng/mL) and treated with QXJYF granules (0.5, 1 mg/mL) *in vitro*. The expression of

M1 macrophage-specific markers (inos, Tnf $\alpha$ , Il1 $\beta$  and Il6) were examined. Data showed that QXJYF treatment significantly reduced the mRNA expression levels of M1 genes, such as inos, Tnf $\alpha$ , Il1 $\beta$  and Il6, in comparison to M1 macrophages (Fig. 6A). Flow cytometry analysis further revealed that the presence of iNOS<sup>+</sup> and TNF $\alpha$ <sup>+</sup> macrophages was increased after stimulation with LPS and IFN $\gamma$ , but significantly decreased in QXJYF-treated BMDMs compared to M1 macrophages (Fig. 6B). To sum up, these findings suggest that QXJYF granules had modulatory effect on macrophage polarization, inhibiting the pro-inflammatory M1 macrophages during AP both *in vivo* and *in vitro*.



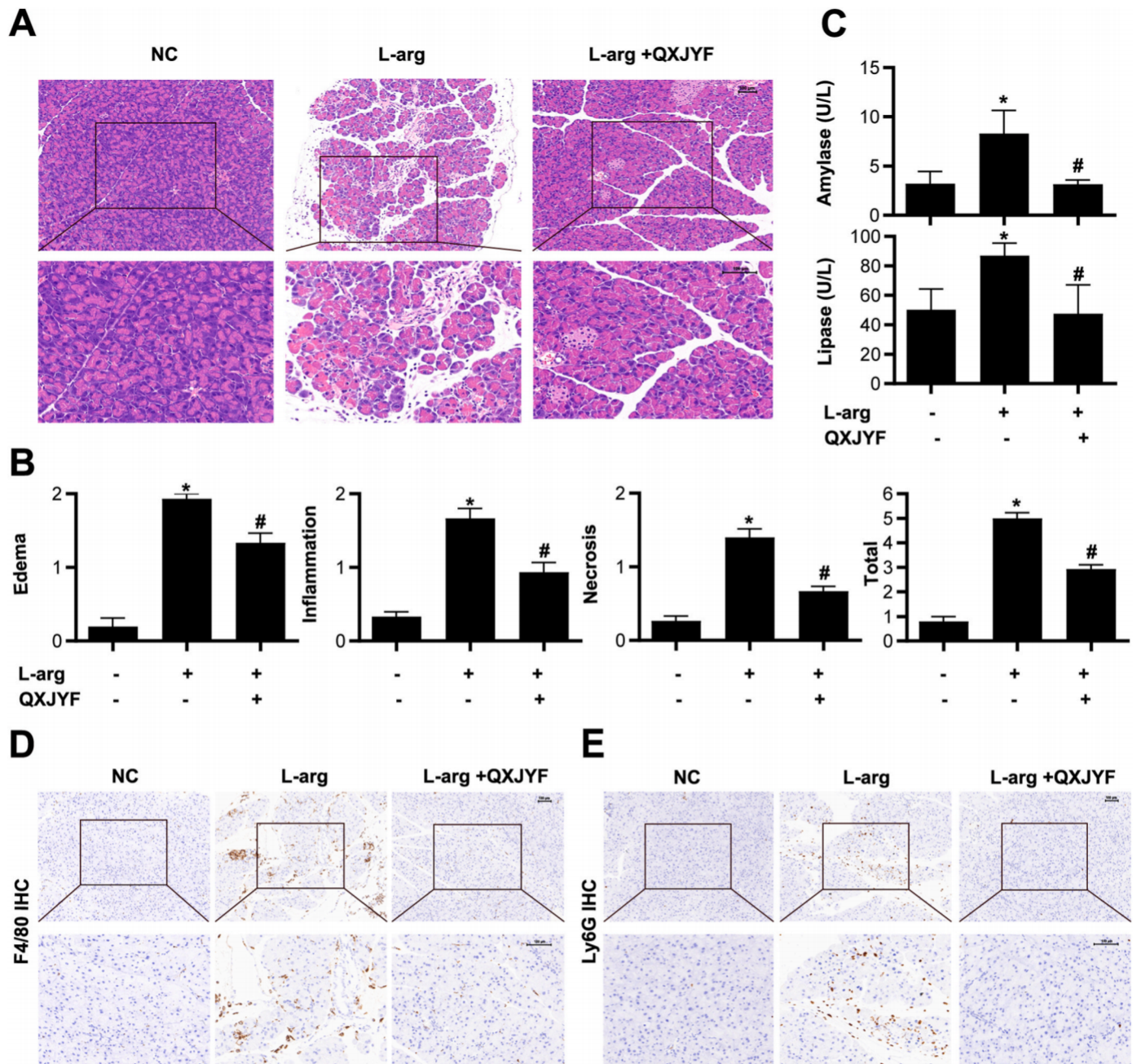


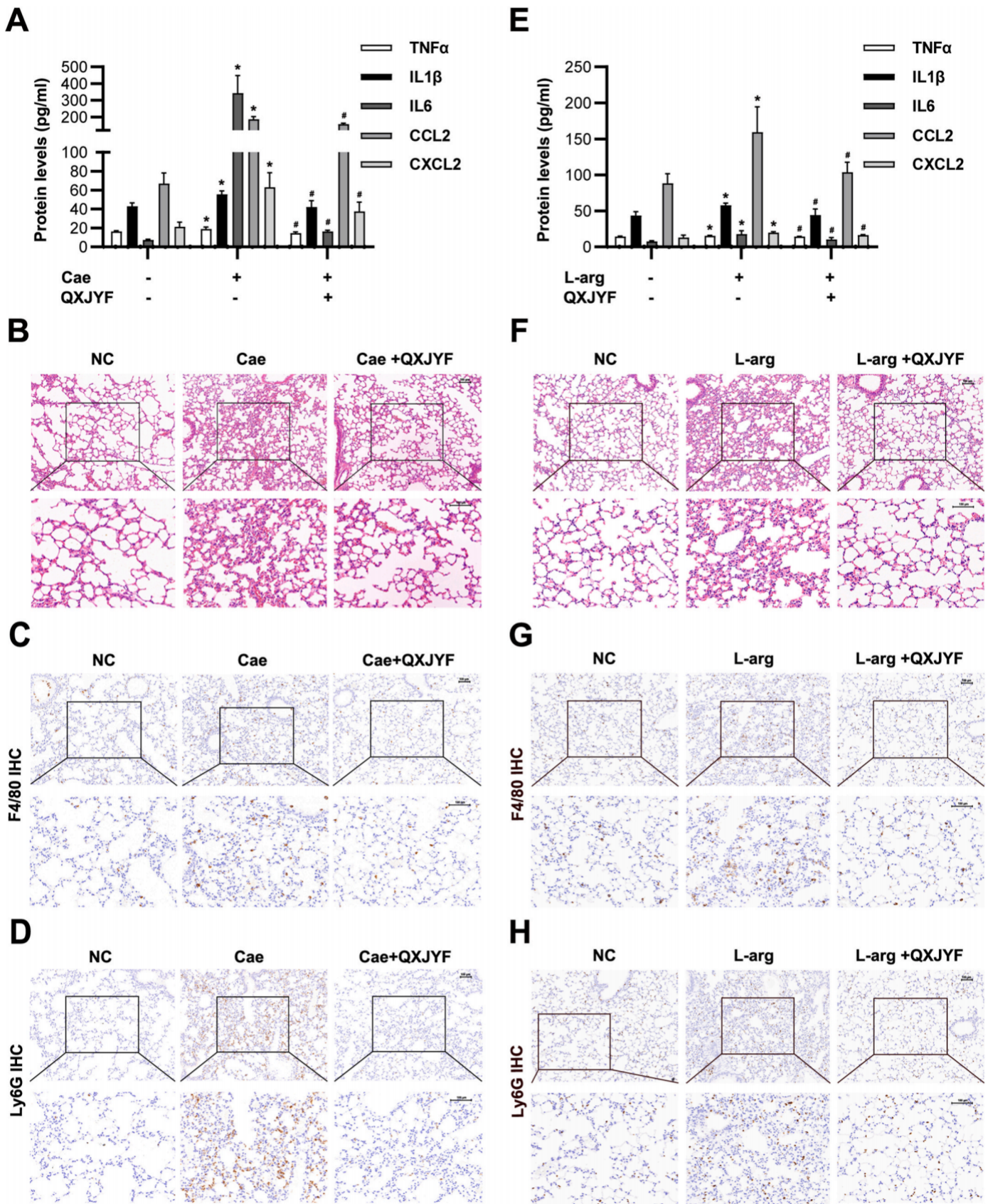
**Fig. 3.** QXJYF granules alleviated pancreas injury in L-arginine-induced AP model. *In vivo*, AP was induced by injection of L-arginine (10 mg/kg) in C57BL/6J mice, and treated with QXJYF granules (4.8 mg/g, 0.6 ml, i.g; at 2 h before and 1 h after the first L-arginine injection respectively). (A) Representative micrographs of H&E-stained pancreatic sections (100 × (up) and 200 × (down)); (B) Histological scores were determined as described in Methods; (C) Change in serum activity of amylase (up) and lipase (down); (D) Representative micrographs of macrophage marker F4/80 immunohistochemical analyses in pancreas (100 × (up) and 200 × (down)); (E) Representative micrographs of neutrophil marker Ly6G immunohistochemical analyses in pancreas (100 × (up) and 200 × (down)). All experiments were performed at least three times. Data are presented as mean ± SEM. n = 9 per group. Scale bar = 100 μm \*P < 0.05 versus NC, #P < 0.05 versus AP. L-arg, L-arginine; NC, normal control; QXJYF, Qing Xia Jie Yi Formula; i.g, intragastric administration.

### 3.5. QXJYF granules inhibited M1 macrophage polarization by suppressing glycolysis during AP

Accumulating evidence has revealed that cellular metabolic adaptation is a critical characteristic of macrophages in supporting their different polarization status and its functions. It has been observed that M1 macrophages primarily rely on glycolysis as their metabolic pathway to stimulate the production of inflammatory mediators (Yuan and Fan, 2022). Conversely, M2 macrophages require a continuous energy supply from fatty acid oxidation and glucose oxidation metabolism to promote wound healing and tissue repair (Wang, F. et al., 2018). Furthermore,

the regulation of these metabolic pathways, either through genetic or pharmacological interventions, can influence the polarization status of macrophages. In this particular study, our aim was to investigate whether the use of QXJYF granules could modulate the functions of M1 macrophages by regulating glycolysis during AP. As expected, our qRT-PCR analysis revealed that the mRNA levels of glycolysis-related enzymes, including Hk2, Pfkfb3, Pkm and Ldhα mRNA levels were significantly increased in LPS and IFNγ-induced M1 macrophages. However, when treated with QXJYF granules, we observed a concentration-dependent decrease in the mRNA levels of these enzymes (Fig. 7A). Consistently, Western blot analysis also demonstrated that the





(caption on next page)



**Fig. 4.** QXJYF granules alleviated systemic injury both in caerulein and L-arginine-induced AP models. (A–D) *In vivo*, AP was induced by injection of caerulein (100 µg/kg) in C57BL/6J mice, and treated with QXJYF granules (4.8 mg/g, 0.6 ml, i.g; at 3 h, 5 h and 7 h after the first caerulein injection respectively). (A) ELISA of serum TNFα, IL1β, IL6, CCL2 and CXCL2 in caerulein-induced AP model; (B) Representative micrographs of H&E-stained lung sections (100 × (up) and 200 × (down)) in caerulein-induced AP model; (C) Representative micrographs of macrophage marker F4/80 immunohistochemical analyses in lung (100 × (up) and 200 × (down)) in caerulein-induced AP model; (D) Representative micrographs of neutrophil marker Ly6G immunohistochemical analyses in lung (100 × (up) and 200 × (down)) in caerulein-induced AP model. (E–H) *In vivo*, AP was induced by injection of L-arginine (10 mg/kg) in C57BL/6J mice, and treated with QXJYF granules (4.8 mg/g, 0.6 ml, i.g; at 2 h before and 1 h after the first L-arginine injection respectively). (E) ELISA of serum TNFα, IL1β, IL6, CCL2 and CXCL2 in L-arginine-induced AP model; (F) Representative micrographs of H&E-stained lung sections (100 × (up) and 200 × (down)) in L-arginine-induced AP model; (G) Representative micrographs of macrophage marker F4/80 immunohistochemical analyses in lung (100 × (up) and 200 × (down)) in L-arginine-induced AP model; (H) Representative micrographs of neutrophil marker Ly6G immunohistochemical analyses in lung (100 × (up) and 200 × (down)) in L-arginine-induced AP model. All experiments were performed at least three times. Data are presented as mean ± SEM. n = 9 per group. Scale bar = 100 µm \*P < 0.05 versus NC, #P < 0.05 versus AP. Cae, caerulein; L-arg, L-arginine; NC, normal control; QXJYF, Qing Xia Jie Yi Formula; i.g, intragastrical administration.

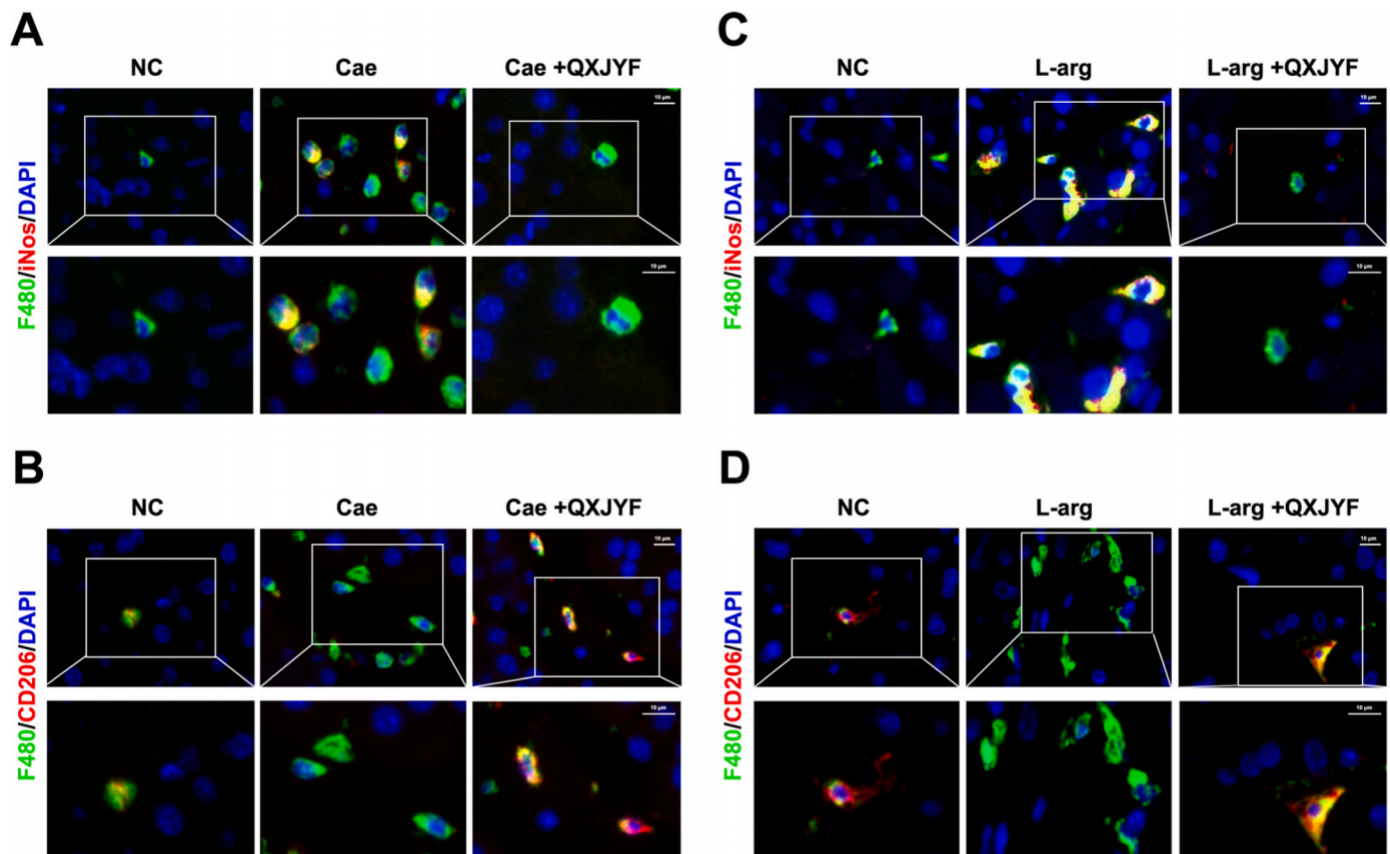


**Fig. 5.** QXJYF granules inhibited M1 macrophage of pancreatic tissue both in caerulein and L-arginine-induced AP model *in vivo*. (A, B) *In vivo*, AP was induced by injection of caerulein (100 µg/kg) in C57BL/6J mice, and treated with QXJYF granules (4.8 mg/g, 0.6 ml, i.g; at 3 h, 5 h and 7 h after the first caerulein injection respectively). (A) Representative micrographs of iNOS with macrophage marker F4/80 immunofluorescence analyses in pancreas during caerulein-induced AP. (B) Representative micrographs of CD206 with macrophage marker F4/80 immunofluorescence analyses in pancreas during caerulein-induced AP. (C, D) *In vivo*, AP was induced by injection of L-arginine (10 mg/kg) in C57BL/6J mice, and treated with QXJYF granules (4.8 mg/g, 0.6 ml, i.g; at 2 h before and 1 h after the first L-arginine injection respectively). (C) Representative micrographs of iNOS with macrophage marker F4/80 immunofluorescence analyses in pancreas during L-arginine-induced AP. (D) Representative micrographs of CD206 with macrophage marker F4/80 immunofluorescence analyses in pancreas during L-arginine-induced AP. Cae, caerulein; L-arg, L-arginine; NC, normal control; QXJYF, Qing Xia Jie Yi Formula; i.g, intragastrical administration.

protein levels of HK2, PFKFB3, PKM and LDHα levels were increased in M1 macrophages but significantly decreased after QXJYF treatment (Fig. 7B). In conclusion, these data suggested that the administration of QXJYF granules could alleviate AP through inhibition of M1 macrophage polarization by suppressing glycolysis (Fig. 7C).

### 3.6. QXJYF granules prevented pSAP patients progressing to SAP

To evaluate the impact of early application of QXJYF granules on the severity and progression of AP patients, a total of 127 pSAP patients were recruited according to the inclusion and exclusion criteria. Among them, 55 patients were in the control group and 72 patients were in the

treatment group. There was no statistical difference in the basic information and baseline characteristics between the two groups: basic information including age, sex, severity, etiology and previous history; baseline characteristics including the CRP level, SIRS score, PASS score and APACHE II score at day0 (Table 1). There was no statistical significance in the level of serum CRP at the 1st day between the control group and the treatment group ( $P > 0.05$ ), while the levels of serum CRP at the 3rd, 7th and 14th day in the treatment group were lower than those in the control group significantly ( $P < 0.05$ , Fig. 8A). The PASS score at the 3rd and 7th day in the treatment group were significantly lower than those in the control group ( $P < 0.05$ ), and PASS score of both groups decreased to 0 at the 14th day (Fig. 8B). However, there was no

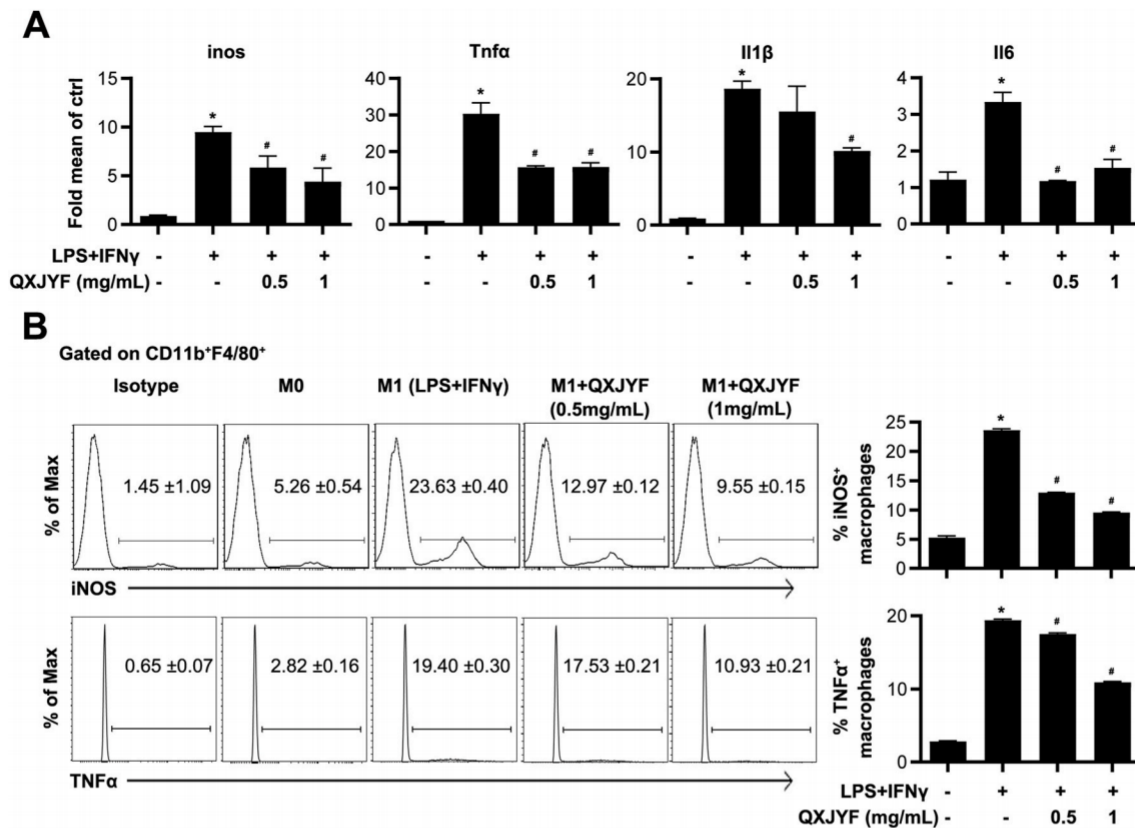


Fig. 6. QXJYF granules inhibited M1 macrophage polarization *in vitro*. M1 macrophages were induced by 100 ng/ml LPS and 10 ng/ml IFN $\gamma$  and were treated with QXJYF granules (0.5, 1 mg/mL) at the same time. (A) mRNA levels of inos, Tnfa, Il1 $\beta$ , and Il6 by qRT-PCR in LPS and IFN $\gamma$ -stimulated BMDMs. (b) FCM of iNOS and TNF $\alpha$  expression in LPS and IFN- $\gamma$ -stimulated BMDMs. n = 9 per group, data were expressed as mean  $\pm$  SEM. \* $P$  < 0.05 versus NC; # $P$  < 0.05 versus LPS and IFN- $\gamma$ .

significant difference in SIRS occurrence, APACHE II score, length of stay and hospitalization cost between the two groups (Table 2). As shown in Table 3, after 7 days of treatment, a total of 36 cases of pSAP progressed to SAP (28.35%), including 22 cases in the control group and 14 cases in the treatment group; compared with the control group, the incidence of SAP in the treatment group was significantly decreased (19.44% vs 40.00%,  $\chi^2 = 4.33$ ,  $P < 0.05$ ). There was no significant difference in the number of people with organ failure (OF) between the two groups. However, more patients in the treatment group had transient OF (<48h) than in the control group (64.10% vs 31.25%,  $\chi^2 = 4.70$ ,  $P < 0.05$ ), and more patients had persistent OF (>48h) in the control group (35.89% vs 68.75%,  $\chi^2 = 4.70$ ,  $P < 0.05$ ). These results indicated that QXJYF granules could significantly reduce CRP levels and shorten the duration of OF, thereby reducing the incidence of SAP, that is, preventing pSAP patients progressing to SAP.

#### 4. Discussion

During AP, macrophages are the prevailing type of immune cells infiltrated into pancreas at the early phase, and are the most abundant immune cells in pancreatic tissue at the regenerative phase (Manohar et al., 2021; Wu et al., 2020). Therefore, macrophages are crucial in the development and progression of AP; however, their phenotype and regulation mode in pancreatic tissue has not been fully elucidated (Cruz and Rohban, 2020). In general, macrophages can be roughly divided into two phenotypes based on different stimuli and function: (1) classically activated macrophages (M1 type), which can be induced by IFN $\gamma$  and/or LPS, are characterized by the production of reactive oxygen species and playing a vital role in inflammatory response; (2) alternatively activated macrophages (M2 type), which can be induced by IL4 and/or IL13, are characterized by the expression of the scavenger

receptor CD206 on the cell surface and involved in inflammatory repair, wound healing, fibrosis or tumorigenesis (Orecchioni et al., 2019; Wang, Y. et al., 2018). Macrophages have the ability to switch their functional phenotypes based on different local microenvironmental signals. This phenotypic switch plays a crucial role in orchestrating the inflammation, repair and regeneration processes following AP injury (Lu and Lu, 2021; Wu et al., 2020). During the initial stage of AP, injured acinar cells release damage-associated molecular patterns (DAMPs) which exacerbate pancreatitis by recruiting immune cells. This leads to the rapid activation of M1 macrophages and the progression of AP through the release of inflammatory cytokines (Tang et al., 2022). M1-type macrophages dominated in the acute inflammatory phase of AP, while M2 macrophages dominated during the process of pancreas repair or regeneration (Wu et al., 2020). Therefore, regulating the macrophage phenotype can be a potential therapeutic strategy for AP.

Here in this study, we conducted research on QXJYF granules, an improved prescription in TCM. We utilized UPLC-Q-Orbitrap MS to identify the major compounds present in QXJYF granules. Our findings demonstrated that the administration of QXJYF granules had a significant impact on alleviating pancreas injury and systemic injury during AP, as observed both in caerulein and L-arginine-induced AP models. Then we illustrated the effects of QXJYF granules on macrophage phenotype from three perspectives: firstly, the results of immunofluorescence staining data indicated that QXJYF granules significantly inhibited F4/80<sup>+</sup>iNOS<sup>+</sup> M1 macrophages while promoting the presence of F4/80<sup>+</sup>CD206<sup>+</sup> M2 macrophages in the pancreatic tissue both in caerulein and L-arginine-induced AP models; secondly, qRT-PCR analysis provided insights into the mRNA expression levels of M1 genes such as inos, Tnfa, Il1 $\beta$  and Il6 were significantly lower after administration of QXJYF granules compared to M1 macrophages stimulated by LPS and IFN $\gamma$ ; last but not least, flow cytometry analysis also revealed that iNOS<sup>+</sup>



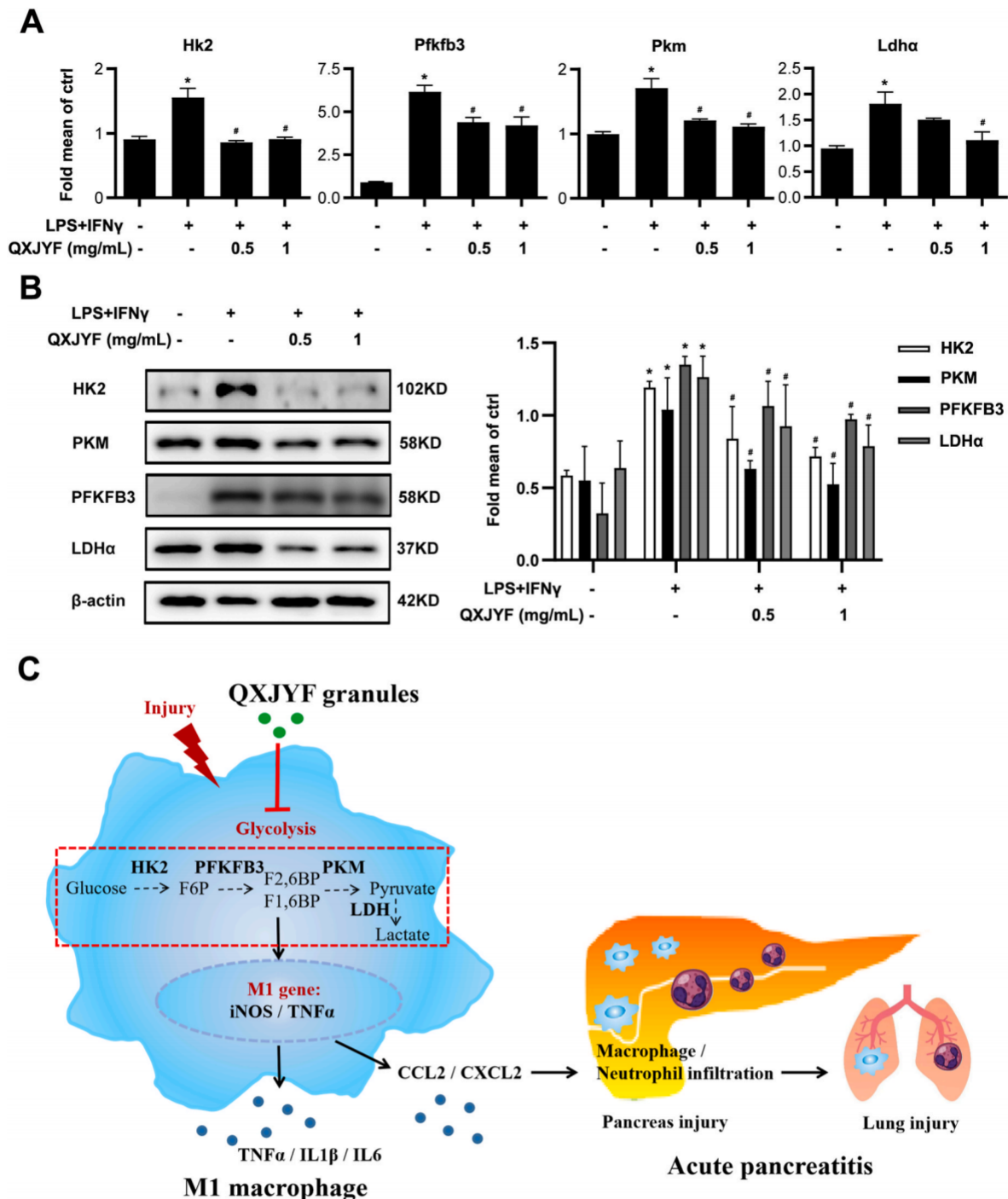


**Fig. 7.** QXJYF granules inhibited M1 macrophage polarization by suppressing glycolysis during AP. M1 macrophages were induced by 100 ng/ml LPS and 10 ng/ml IFN $\gamma$  and were treated with QXJYF granules (0.5, 1 mg/mL) at the same time. (A) mRNA levels of Hk2, Pfkfb3, Pkm and Ldh $\alpha$  by qRT-PCR in LPS and IFN $\gamma$ -stimulated BMDMs; (B) Immunoblot analysis of HK2, PKM, PFKFB3 and LDH $\alpha$  levels in LPS and IFN $\gamma$ -stimulated BMDMs; (C) Schematic diagram summarized the effect of QXJYF granules on macrophage polarization by suppressing glycolysis in experimental acute pancreatitis. n = 9 per group, data were expressed as mean  $\pm$  SEM. \* $P$  < 0.05 versus NC; # $P$  < 0.05 versus LPS and IFN- $\gamma$ .

and TNF $\alpha$ <sup>+</sup> macrophages were significantly reduced after QXJYF treatment in comparison to LPS and IFN $\gamma$ -stimulated M1 macrophages. To sum up, our study showed that QXJYF granules effectively alleviated AP through inhibition of M1 macrophage polarization both *in vivo* and *in vitro*.

Macrophages significantly alter their metabolic pathways when their polarization state changes. Under the stimulation of LPS, IFN $\gamma$  or IL12, macrophages shift their metabolism to glycolysis pathway. LPS and IFN $\gamma$  had been found to stimulate glucose uptake by macrophages while

inhibiting fatty acid uptake or oxidation. In other words, M1 macrophages rely on glycolysis for ATP production and increase their consumption of glucose, but they suppress oxidative metabolism (Liu et al., 2017). Glycolysis is a complex process consisting of ten steps, starting with a single glucose molecule and resulting in the production of two pyruvate molecules, involving several rate-limiting enzymes including HK2, PFKFB3 and PKM; and pyruvate can be reduced to lactic acid under the catalysis of LDH $\alpha$  in hypoxia conditions (Naifeh et al., 2023). However, the specific mechanisms and target of glycolysis regulating

**Table 1**  
Basic information of AP patients.

	Treatment group (n = 72)	Control group (n = 55)	P value
Age (mean ± SD)	53.4 ± 15.7	46.7 ± 15.1	0.106
Gender			0.905
Male (n, %)	53(73.6)	41 (74.5)	
Female (n, %)	19 (26.4)	14 (25.5)	
AP severity			0.066
MAP (n, %)	45 (62.5)	42 (76.4)	
MSAP (n, %)	23 (31.9)	8 (14.5)	
SAP (n, %)	4 (5.6)	5 (9.1)	
AP etiology			0.472
Biliary (n, %)	31 (47.0)	27 (54.0)	
Hyperlipidemic (n, %)	22 (33.3)	14 (28.0)	
Alcoholic (n, %)	9 (13.6)	4 (8.0)	
Infection (n, %)	0 (0)	1 (2.0)	
Endocrine/metabolic (n, %)	1 (1.5)	3 (6.0)	
Others (n, %)	3 (4.5)	1 (2.0)	
BMI (kg/m <sup>2</sup> )			0.080
<25 (n, %)	34 (47.2)	16 (29.1)	
25 to 30 (n, %)	26 (36.1)	23 (41.8)	
≥30 (n, %)	12 (16.7)	16 (29.1)	
Balthazar CT score			0.286
2 (n, %)	47 (65.3)	39 (70.9)	
4 (n, %)	22 (30.6)	11 (20.0)	
6 (n, %)	3 (4.2)	5 (9.1)	
Baseline CRPD0 (M, IQR)*	25.3 (5.6, 109.1)	37.0 (12.2, 110.9)	0.315
Baseline PASS score D0 (M, IQR)*	48 (45, 72)	56 (45, 82.5)	0.303
Baseline SIRS score D0			0.229
0 (n, %)	36 (50.0)	27 (49.1)	
1 (n, %)	25 (34.7)	17 (30.9)	
2 (n, %)	9 (12.5)	7 (12.7)	
3 (n, %)	2 (2.8)	2 (3.6)	
4 (n, %)	0(0)	2 (3.6)	
Baseline APACHE II score D0	34 ± 14	36 ± 11	0.594

\*P < 0.05.

macrophage polarization during AP have not been fully elucidated. In this study, we detected the protein and mRNA levels of HK2, PFKFB3, PKM and LDHα by Western blot and qRT-PCR. Our data showed that after M0 macrophages differentiated into M1 phenotype, HK2, PFKFB3, PKM and LDHα expression level significantly increased, suggesting that glycolytic metabolism increased in M1 macrophages. However, QXJYF granules inhibited these enzymes of glycolysis in M1 macrophages. Furthermore, recent reports have highlighted the vital role of glycolysis in activated macrophages (Edgar and Akbar, 2021). Genetic or pharmacological intervention of glycolysis can regulate the phenotype of macrophages. Therefore, combined with the literature and these experimental results, we concluded that QXJYF granules inhibited M1 macrophage polarization by suppressing glycolysis. In addition to AP,

**Table 2**  
Comparison of therapeutic effect between the treatment group and control group.

	Treatment group (n = 72)	Control group (n = 55)	P value
CRP D1 (M, IQR)*	91.0 (22.0, 188.6)	98.5 (22.7, 190.1)	0.782
CRP D3 (M, IQR)*	48.4 (14.6, 121.2)	98.8 (27.4, 177.1)	0.031*
CRP D7 (M, IQR)*	11.4 (6.7, 53.1)	36.6 (9.5, 118.8)	0.019*
CRP D14 (M, IQR)*	1.3 (1.1, 2.6)	15.4 (10.2, 53.1)	0.002*
PASS score D1 (M, IQR)*	67 (47, 111.75)	72 (46, 93.5)	0.872
PASS score D3(M, IQR)*	43 (40, 65)	47 (43, 74.5)	0.005*
PASS score D7 (M, IQR)*	12 (0, 40)	23.5 (20, 32)	0.027*
PASS score D14 (M, IQR)*	0 (0, 0)	0 (0, 0)	0.361
SIRS score D1			0.032*
0 (n, %)	35 (48.6)	25 (45.5)	
1 (n, %)	15 (20.8)	18 (32.7)	
2 (n, %)	17 (23.6)	4 (7.3)	
3 (n, %)	5 (6.9)	6 (10.9)	
4 (n, %)	0(0)	2 (3.6)	
SIRS score D3			0.196
0 (n, %)	48 (66.7)	33 (60.0)	
1 (n, %)	19 (26.4)	12 (21.8)	
2 (n, %)	4 (5.6)	4 (7.3)	
3 (n, %)	1 (1.4)	5 (9.1)	
4 (n, %)	0(0)	1 (1.8)	
SIRS score D7			0.258
0 (n, %)	61 (84.7)	43 (78.2)	
1 (n, %)	9 (12.5)	6 (10.9)	
2 (n, %)	2 (2.8)	5 (9.1)	
3 (n, %)	0(0)	1 (1.8)	
4 (n, %)	0(0)	0(0)	
SIRS score D14			0.305
0 (n, %)	61 (98.4)	41 (93.2)	
1 (n, %)	1 (1.6)	3 (6.8)	
2 (n, %)	0(0)	0(0)	
3 (n, %)	0(0)	0(0)	
4 (n, %)	0(0)	0(0)	
APACHE II score D1 (Mean ± SD)	4 ± 3	3 ± 2	0.486
APACHE II score D3 (Mean ± SD)	3 ± 2	3 ± 2	0.573
APACHE II score D7 (Mean ± SD)	3 ± 2	2 ± 2	0.453
APACHE II score D14 (Mean ± SD)	2 ± 2	2 ± 2	0.079
Length of hospitalization (Mean ± SD)	11 ± 5	10 ± 5	0.139
Hospitalization costs (M, IQR)*	15965.9 (10649.9, 21963.6)	22526.9 (12966.9, 27617.6)	0.098

\*P < 0.05.

M1 macrophages are also activated in sepsis and other diseases. Inhibition of M1 macrophages by inhibiting glycolysis can significantly improve the inflammatory response in the process, thereby reducing the severity of these M1 macrophage-related diseases, which has important clinical significance and potential application prospects. Compared with

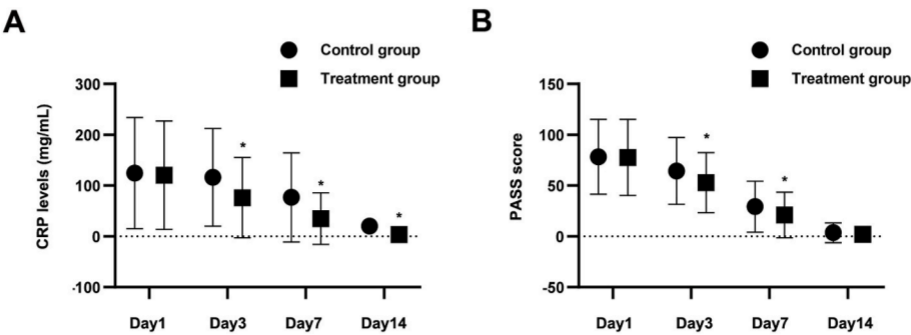


**Fig. 8.** QXJYF treatments reduced CRP and PASS score of AP patients. A total of 127 pSAP patients were recruited: 55 patients were in the control group and 72 patients were in the treatment group. (A) Dynamic change of serum CRP levels in control and treatment group; (B) Dynamic change of PASS score in control and treatment group. \*P < 0.05 versus control group.



**Table 3**  
Difference of OF and SAP between the control and treatment group.

Group	OF (n, %)	OF duration time (n, %)		SAP (n, %)
		<48h	>48h	
Treatment group	39 (54.16)	25 (64.10)	14 (35.89)	14 (19.44)
Control group	32 (58.18)	10 (31.25)	22 (68.75)	22 (40.00)
$\chi^2$ value	0.29	4.70	4.70	4.33
P value	0.59	0.03*	0.03*	0.04*

\*P < 0.05. OF, organ failure; SAP, severe acute pancreatitis.

Western medicine, TCM prescriptions currently used in clinical practice have some shortcomings, such as decocting and taking methods, difficult to control drug concentration, less effective ingredients, longer time consuming, lack of unified judgment indicators and diagnosis or treatment standards. These limitations restrict the effective promotion of TCM. Therefore, we hope that these problems can be gradually solved in clinical practice in the future, and provide practical basis for the better use of TCM in clinical practice.

There were still some shortcomings in this study. Macrophage polarization is closely related to glucose metabolism, fatty acid oxidation, amino acid metabolism and other substances (Biczo et al., 2018; Zhang et al., 2022). The effect of QXJYF granules on the metabolism of other substances except glycolysis is not very clear and needs to be further explored. Besides, the clinical part of this study included a small number of cases, and the sample size can be expanded to further study the therapeutic effect of QXJYF granules on AP.

5. Conclusion

In summary, combining experimental and clinical data, we found that QXJYF granules might reduce the expression of proinflammatory cytokines in M1 macrophages and negatively regulate the polarization of M1 macrophages by inhibiting glycolysis. This study provided a new idea for exploring the immunotherapy of TCM in macrophage-related inflammatory diseases.

CRediT authorship contribution statement

**Xiao Han:** Conceptualization, Data curation, Funding acquisition, Investigation, Methodology, Writing – original draft, Writing – review & editing. **Jingpiao Bao:** Data curation, Writing – original draft. **Jianbo Ni:** Data curation. **Bin Li:** Conceptualization, Formal analysis. **Pengli Song:** Formal analysis, Investigation, Software. **Rong Wan:** Resources, Supervision, Validation. **Xingpeng Wang:** Funding acquisition, Writing – review & editing. **Guoyong Hu:** Funding acquisition, Resources, Supervision, Validation, Visualization, Writing – review & editing. **Congying Chen:** Supervision, Writing – original draft, Writing – review & editing.

Declaration of competing interest

The authors declare that the research was conducted in the absence of any commercial or financial relationships that could be construed as a potential conflict of interest.

Data availability

Data will be made available on request.

Acknowledgment

The study was supported by National Natural Science Foundation of China (No.81900584, XH), Shanghai Traditional Chinese Medicine and Western Clinical Cooperation Pilot Project (No.ZY(2018–2020)-FWTX-1004, XPW) and Clinical Research Plan of SHDC (No.

SHDC2020CR5013, HGY).

Abbreviations

AP	acute pancreatitis
Cae	caerulein
QXJYF	Qing Xia Jie Yi Formula
HK2	Hexokinase 2
H&E	hematoxylin and eosin
LDHα	lactic dehydrogenase α
LPS	lipopolysaccharide
L-arg	L-arginine
NS	normal saline
PFKFB3	Fructose-2, 6-diphosphatase 3
PKM	pyruvate kinase
pSAP	predicted severe acute pancreatitis
SAP	severe acute pancreatitis
TCM	Traditional Chinese Medicine.

Appendix A. Supplementary data

Supplementary data related to this article can be found at <http://doi.org/10.1016/j.jep.2024.117750>.

References

Anthony, R.M., Kobayashi, T., Wermeling, F., Ravetch, J.V., 2011. Intravenous gammaglobulin suppresses inflammation through a novel T(H)2 pathway. *Nature* 475 (7354), 110–113.

Banks, P.A., Bollen, T.L., Dervenis, C., Gooszen, H.G., Johnson, C.D., Sarr, M.G., Tsiotis, G.G., Vege, S.S., 2013. Classification of acute pancreatitis–2012: revision of the Atlanta classification and definitions by international consensus. *Gut* 62 (1), 102–111.

Bi, S., Liu, Y., Lv, T., Ren, Y., Liu, K., Liu, C., Zhang, Y., 2023. Preliminary exploration of method for screening efficacy markers compatibility in TCM prescriptions based on Q-markers: anti-inflammatory activity of Dachaihu decoction as an example. *J. Ethnopharmacol.* 312, 116539.

Biczo, G., Vegh, E.T., Shalbueva, N., Mareninova, O.A., Elperin, J., Lotshaw, E., Gretler, S., Lugea, A., Malla, S.R., Dawson, D., Ruchala, P., Whitelegge, J., French, S.W., Wen, L., Husain, S.Z., Gorelick, F.S., Hegyi, P., Rakonczay Jr., Z., Gukovsky, I., Gukovskaya, A.S., 2018. Mitochondrial dysfunction, through impaired autophagy, leads to endoplasmic reticulum stress, deregulated lipid metabolism, and pancreatitis in animal models. *Gastroenterology* 154 (3), 689–703.

Buxbaum, J., Quezada, M., Chong, B., Gupta, N., Yu, C.Y., Lane, C., Da, B., Leung, K., Shulman, I., Pandol, S., Wu, B., 2018. The Pancreatitis Activity Scoring System predicts clinical outcomes in acute pancreatitis: findings from a prospective cohort study. *Am. J. Gastroenterol.* 113 (5), 755–764.

Chen, W., Yang, X., Huang, L., Xue, P., Wan, M., Guo, J., Zhu, L., Jin, T., Huang, Z., Chen, G., Tang, W., Xia, Q., 2015. Qing-Yi decoction in participants with severe acute pancreatitis: a randomized controlled trial. *Chin. Med.* 10, 11.

Cruz, A.F., Rohban, R., 2020. Macrophages in the pancreas: villains by circumstances, not necessarily by actions. *Immunity. Inflamm. Dis.* 8 (4), 807–824.

Dawra, R., Sharif, R., Phillips, P., Dudeja, V., Dhaulakhandi, D., Saluja, A.K., 2007. Development of a new mouse model of acute pancreatitis induced by administration of L-arginine. *Am. J. Physiol. Gastrointest. Liver Physiol.* 292 (4), G1009–G1018.

Edgar, L., Akbar, N., 2021. Hyperglycemia induces trained immunity in macrophages and their precursors and promotes atherosclerosis. *Circulation* 144 (12), 961–982.

Han, X., Li, B., Bao, J., Wu, Z., Chen, C., Ni, J., Shen, J., Song, P., Peng, Q., Wan, R., Wang, X., Wu, J., Hu, G., 2022. Endoplasmic reticulum stress promoted acinar cell necroptosis in acute pancreatitis through cathepsinB-mediated AP-1 activation. *Front. Immunol.* 13, 968639.

Kim, D.G., Bae, G.S., Choi, S.B., Jo, I.J., Shin, J.Y., Lee, S.K., Kim, M.J., Kim, M.J., Jeong, H.W., Choi, C.M., Seo, S.H., Choo, G.C., Seo, S.W., Song, H.J., Park, S.J., 2015. Guggulsterone attenuates cerulein-induced acute pancreatitis via inhibition of ERK and JNK activation. *Int. Immunopharm.* 26 (1), 194–202.

Lee, D.W., Cho, C.M., 2022. Predicting severity of acute pancreatitis. *Medicina* 58 (6).

Lerch, M.M., Gorelick, F.S., 2013. Models of acute and chronic pancreatitis. *Gastroenterology* 144 (6), 1180–1193.

Liu, P.S., Wang, H., Li, X., Chao, T., Teav, T., Christen, S., Di Conza, G., Cheng, W.C., Chou, C.H., Vavakova, M., Muret, C., Debacquer, K., Mazzone, M., Huang, H.D., Fendt, S.M., Ivanisevic, J., 2017. α-ketoglutarate orchestrates macrophage activation through metabolic and epigenetic reprogramming. *Nat. Immunol.* 18 (9), 985–994.

Lu, Y., Lu, G., 2021. The proresolving lipid mediator Maresin1 alleviates experimental pancreatitis via switching macrophage polarization. *Mediat. Inflamm.* 2021, 6680456.

Manohar, M., Jones, E.K., Rubin, S.J.S., Subrahmanyam, P.B., Swaminathan, G., Mikhail, D., Bai, L., Singh, G., Wei, Y., Sharma, V., Siebert, J.C., Maecker, H.T., Husain, S.Z., Park, W.G., Pandol, S.J., Habtezion, A., 2021. Novel circulating and

- tissue monocytes as well as macrophages in pancreatitis and recovery. *Gastroenterology* 161 (6), 2014-2029.e2014.
- Naifeh, J., Dimri, M., Varacallo, M., 2023. *Biochemistry, aerobic glycolysis*, StatPearls. In: StatPearls Publishing Copyright © 2023. StatPearls Publishing LLC., Treasure Island (FL).
- Orecchioni, M., Ghosheh, Y., Pramod, A.B., Ley, K., 2019. Macrophage polarization: different gene signatures in M1(LPS+) vs. Classically and M2(LPS-) vs. Alternatively activated macrophages. *Front. Immunol.* 10, 1084.
- Sah, R.P., Dudeja, V., Dawra, R.K., Saluja, A.K., 2013. Cerulein-induced chronic pancreatitis does not require intra-acinar activation of trypsinogen in mice. *Gastroenterology* 144 (5), 1076-1085. .e1072.
- Szatmary, P., Grammatikopoulos, T., Cai, W., Huang, W., Mukherjee, R., Halloran, C., Beyer, G., Sutton, R., 2022. Acute pancreatitis: diagnosis and treatment. *Drugs* 82 (12), 1251-1276.
- Tang, D., Cao, F., Yan, C., Fang, K., Ma, J., Gao, L., Sun, B., Wang, G., 2022. Extracellular vesicle/macrophage Axis: potential targets for inflammatory disease intervention. *Front. Immunol.* 13, 705472.
- Tarasziuk, A., Bulak, K., Talar, M., Fichna, J., 2021. Chlorogenic acid reduces inflammation in murine model of acute pancreatitis. *Pharmacol. Rep. : PR* 73 (5), 1448-1456.
- Van Laethem, J.L., Marchant, A., Delvaux, A., Goldman, M., Robberecht, P., Velu, T., Devière, J., 1995. Interleukin 10 prevents necrosis in murine experimental acute pancreatitis. *Gastroenterology* 108 (6), 1917-1922.
- Vege, S.S., Atwal, T., Bi, Y., Chari, S.T., Clemens, M.A., Enders, F.T., 2015. Pentoxifylline treatment in severe acute pancreatitis: a Pilot, double-blind, placebo-controlled, randomized trial. *Gastroenterology* 149 (2), 318-320. .e313.
- Wang, F., Zhang, S., Vuckovic, I., Jeon, R., Lerman, A., Folmes, C.D., Dzeja, P.P., Herrmann, J., 2018. Glycolytic stimulation is not a requirement for M2 macrophage differentiation. *Cell Metabol.* 28 (3), 463-475. .e464.
- Wang, Y., Xu, Y., Zhang, P., Ruan, W., Zhang, L., Yuan, S., Pang, T., Jia, A.Q., 2018. Smiglaside A ameliorates LPS-induced acute lung injury by modulating macrophage polarization via AMPK-PPAR $\gamma$  pathway. *Biochem. Pharmacol.* 156, 385-395.
- Wei, T.F., Zhao, L., Huang, P., Hu, F.L., Jiao, J.Y., Xiang, K.L., Wang, Z.Z., Qu, J.L., Shang, D., 2021. Qing-yi decoction in the treatment of acute pancreatitis: an integrated approach based on chemical profile, network pharmacology, molecular docking and experimental evaluation. *Front. Pharmacol.* 12, 590994.
- Wen, L., Voronina, S., Javed, M.A., Awais, M., Szatmary, P., Latawiec, D., Chvanov, M., Collier, D., Huang, W., Barrett, J., 2015. Inhibitors of ORAI1 prevent cytosolic calcium-associated injury of human pancreatic acinar cells and acute pancreatitis in 3 mouse models. *Gastroenterology* 149 (2), 481.
- Wen, Y., Han, C., Liu, T., Wang, R., Cai, W., Yang, J., Liang, G., Yao, L., Shi, N., Fu, X., Deng, L., Sutton, R., Windsor, J.A., Hong, J., Phillips, A.R., Du, D., Huang, W., Xia, Q., 2020. Chaijin chengqi decoction alleviates severity of acute pancreatitis via inhibition of TLR4 and NLRP3 inflammasome: identification of bioactive ingredients via pharmacological sub-network analysis and experimental validation. *Phytomedicine : Inter. J. Phytother. Phytopharm.* 79, 153328.
- Wu, J., Zhang, L., Shi, J., He, R., Yang, W., Habtezion, A., Niu, N., Lu, P., Xue, J., 2020. Macrophage phenotypic switch orchestrates the inflammation and repair/regeneration following acute pancreatitis injury. *EBioMedicine* 58, 102920.
- Wu, X., Yao, J., Hu, Q., Kang, H., Miao, Y., Zhu, L., Li, C., Zhao, X., Li, J., Wan, M., Tang, W., 2022. Emodin ameliorates acute pancreatitis-associated lung injury through inhibiting the alveolar macrophages pyroptosis. *Front. Pharmacol.* 13, 873053.
- Xue, J., Sharma, V., Hsieh, M.H., Chawla, A., Murali, R., Pandol, S.J., Habtezion, A., 2015. Alternatively activated macrophages promote pancreatic fibrosis in chronic pancreatitis. *Nat. Commun.* 6, 7158.
- Yang, X., Zhang, X., Lin, Z., Guo, J., Yang, X., Yao, L., Wang, H., Xue, P., Xia, Q., 2020. Chaijin chengqi decoction alleviates severe acute pancreatitis associated acute kidney injury by inhibiting endoplasmic reticulum stress and subsequent apoptosis. *Biomed. Pharmacother. = Biomed. Pharmacother.* 125, 110024.
- Ying, W., Cheruku, P.S., Bazer, F.W., Safe, S.H., Zhou, B., 2013. Investigation of macrophage polarization using bone marrow derived macrophages. *J. Vis. Exp.* 76.
- Yuan, Y., Fan, G., 2022. The transcription factor KLF14 regulates macrophage glycolysis and immune function by inhibiting HK2 in sepsis. *Cell. Mol. Immunol.* 19 (4), 504-515.
- Zhang, L., Shi, J., Du, D., Niu, N., Liu, S., Yang, X., Lu, P., Shen, X., Shi, N., Yao, L., Zhang, R., Hu, G., Lu, G., Zhu, Q., Zeng, T., Liu, T., Xia, Q., Huang, W., Xue, J., 2022. Ketogenesis acts as an endogenous protective programme to restrain inflammatory macrophage activation during acute pancreatitis. *EBioMedicine* 78, 103959.
- Zhang, X., Gao, T., Wang, Y., 2019. Geniposide alleviates lipopolysaccharide (LPS)-induced inflammation by downregulation of miR-27a in rat pancreatic acinar cell AR42J. *Biol. Chem.* 400 (8), 1059-1068.